3D-Printed Optical Elements for Coupling of VCSEL and Photodiode Arrays to Multi-Core Fibers in an SFP Transceiver Assembly

Pascal Maier[1,2,*], Yilin Xu[1,2,*], Matthias Lauermann[3], Alexandra Henniger-Ludwig[4], Hermann Kapim[4], Mareike Trappen[1,2], Torben Kind[5], Achim Weber[5], Matthias Blaicher[1,2], Philipp-Immanuel Dietrich[1,2,3], Clemens Wurster[6], Sebastian Randel[1], Wolfgang Freude[1], Christian Koos[1,2,3]

[1] Institute of Photonics and Quantum Electronics (IPQ), Karlsruhe Institute of Technology (KIT), Engesserstr. 5, 76131 Karlsruhe, Germany
[2] Institute of Microstructure Technology (IMT), KIT, Hermann-von-Helmholtz-Platz 1, 76344 Eggenstein-Leopoldshafen, Germany
[3] Vanguard Automation GmbH, Gablonzerstr. 10, 76185 Karlsruhe, Germany
[4] Rosenberger Hochfrequenztechnik GmbH & Co. KG, Hauptstr. 1, 83413 Fridolfing, Germany
[5] ficonTEC Service GmbH, Im Finigen 3, 28832 Achim, Germany
[6] Rosenberger OSI GmbH & Co. OHG, Endorferstr. 6, 86167 Augsburg, Germany
[*] P. Maier and Y. Xu contributed equally to this work
pascal.maier@kit.edu, yilin.xu@kit.edu, christian.koos@kit.edu

Abstract: We demonstrate a 3 × 25 Gbit/s SFP transceiver assembly using 3D-printed optical coupling elements to connect multimode multi-core fibers to linear VCSEL and photodiode arrays. Passive alignment yields average coupling losses below 0.7 dB, ensuring conformity with the IEEE 802.3 power budget. © 2022 The Author(s)

1. Introduction

In recent years, increasing throughput of optical communication systems has primarily relied on higher symbol rates and advanced modulation formats. Giving the steadily rising demand for communication bandwidth, however, the limits of these approaches are becoming increasingly obvious [1,2], especially for short-reach intra-datacenter links, where cost- and energy-efficient implementation is key. Parallel transmission via spatially separated channels is seen as an attractive alternative for bandwidth scaling with linearly increasing technical effort [2]. To maintain the associated fiber installations manageable, notable effort has been spent to replace commonly used fiber ribbons by more compact multi-core fibers (MCF) [3–8]. However, low-loss coupling of light between MCF and standard linear arrays of vertical-cavity surface-emitting lasers (VCSEL) or photodiodes (PD) still remain challenging. Current solutions either rely on fan-out structures to connect the cores of an MCF to individual fibers by fused fiber couplers [5,6] or require device arrays in non-standard 2D arrangements that are precisely matched to the cross-section of the respective MCF [4,7,8]. These solutions are technologically complex and challenging to scale, in particular when it comes to compact short-reach data-center transceivers that are subject to stringent constraints in footprint and in assembly costs.

In this paper, we show that 3D-printed optical elements can be used for efficiently coupling individual cores of multi-mode MCF (MM-MCF) to VCSEL or PD that are arranged in linear arrays with a standard pitch of 250 µm. The freeform coupling elements are fabricated directly on the fiber and device facets by multi-photon lithography and can be designed to provide large alignment tolerance in subsequent passive assembly steps. In a proof-of-concept experiment, we demonstrate average coupling losses of 0.7 dB for the transmitter and 0.6 dB for the receiver side, along with lateral 1 dB alignment tolerances of ±18 µm and ±13 µm for the *x*- and *y*-direction, respectively. To the best of our knowledge, this corresponds to the lowest coupling loss and the highest alignment tolerance so far demonstrated for coupling to MM-MCF. We demonstrate the viability of the concept by integrating our coupling structures into a 3 × 25 Gbit/s transceiver assembly that is compatible with the space requirements of a small form-factor pluggable (SFP) module, and which is in conformity to industry-standard IEEE 802.3 power budget specifications.

2. Coupling concept

The concept of exploiting 3D-printed optical elements for coupling between MM-MCF and linear VCSEL or PD arrays is illustrated in Fig. 1ⓐ. All devices are mounted on a printed circuit board (PCB), which also contains the associated driver electronics, and which is designed to fit into a standard quad SFP (QSFP) module. The transceiver assembly comprises a first MM-MCF for the transmitter (Tx) and a second MM-MCF for the receiver (Rx). Both fibers (OFS MCF-MM-7-39) are glued into a common industry-standard mechanical transfer (MT) ferrule. At the Tx, Fig. 1ⓑ, three VCSEL #1, #2, #3 (Broadcom AFCD-V64JZ, $\lambda = 850\,\text{nm}$) of a linear array of four devices are coupled to three horizontally arranged cores (diameter 26 µm) of the Tx fiber. Both the VCSEL and the fiber facets are equipped with 3D-printed freeform coupling elements, which are referred to as facet-attached microlenses (FaML) in the following. On the VCSEL side, the various FaML are designed to emit a collimated beam towards the respective fiber core. These beams are picked up by a corresponding FaML on the fiber side, each consisting of a 45° mirror and three refractive surfaces. A micrograph of an exemplary FaML on one of the VCSEL is shown in Inset (i) of Fig. 1ⓑ. At the Rx, Fig. 1ⓒ, three PD #4, #5, #6 in a linear array of four devices (Broadcom SPD2025-4X, responsivity $S = 0.5\,\text{A/W}$) are coupled to three horizontally arranged cores of the Rx fiber. In analogy to the Tx side, a first set of FaML on the facets of the fiber cores is used to direct the incoming light towards the respective PD, where a second set of FaML focuses the beams to the sensitive area of the respective device. To compensate for the pitch mismatch between the MM-MCF cores (39 µm) and the VCSEL / PD (250 µm), the outer lenses (Tx #1, #3 in ⓑ; Rx #4, #6 in ⓒ) are rotated by 15°. A technical drawing of a cross-section of Channel #5 in Fig. 1ⓒ is shown in Fig. 1ⓓ. Note that the remaining four cores of the seven-core Tx and Rx MM-MCF are left unused in the current assembly due to space constraints. In principle, these cores could also be connected, e.g., by using more complex coupling structures, possibly in combination with two-dimensional VCSEL and PD arrays.

3. Module assembly

As a first step of the assembly process, we mount the VCSEL and PD array collinearly such that the distance between the respective central channels (#2, #5) matches the distance of 1750 µm between the central cores of the Tx and Rx MM-MCF. The FaML are then printed directly to the fibers, VCSEL, and PD by multi-photon lithography using a negative-tone photoresist with a refractive index $n = 1.54$ at 850 nm. Precise alignment of the FaML relative to the respective facet is ensured by dedicated machine vision techniques. After exposure, the fabricated structures are developed in propylene-glycol-methyl-etheracetate (PGMEA), flushed with isopropanol, and subsequently blow-dried, see Inset (i) of Fig. 1ⓑ for a micrograph of a 3D-printed FaML (lithography system: Sonata 1000, Vanguard Automation GmbH). Subsequently, a custom pick-and-place machine is used to mount the MT ferrule to the PCB in a fully automated process relying solely on camera vision and height measurements by a confocal chromatic imaging sensor (Precitec CHRocodile S [9]). In this step, the MT ferrule is aligned in all six degrees of freedom with respect to the FaML on the VCSEL and PD arrays, see Fig. 1ⓐ and ⓑ. To this end, we first detect the positions of the FaML belonging to the VCSEL of Channel #2 and to the PD of Channel #5 and extract the connecting line. The MT ferrule is then moved in *x*- and *y*-direction to fulfill two criteria: First, two 3D-printed markers with optically detectable holes adjacent to each of the MM-MCF have to fall on top of the previously extracted connecting line. Second, the two FaML at the central MM-MCF cores of the Tx and the Rx fiber must be positioned exactly vertically above the FaML belonging to the VCSEL of Channel #2 and to the PD of Channel #5. Finally, the distance in *z*-direction is adjusted to the designed height using the confocal chromatic imaging sensor. In a final step, the MT ferrule is fixed in this position by an UV-curable epoxy with ultra-low shrinkage (EMI Optocast 3410).

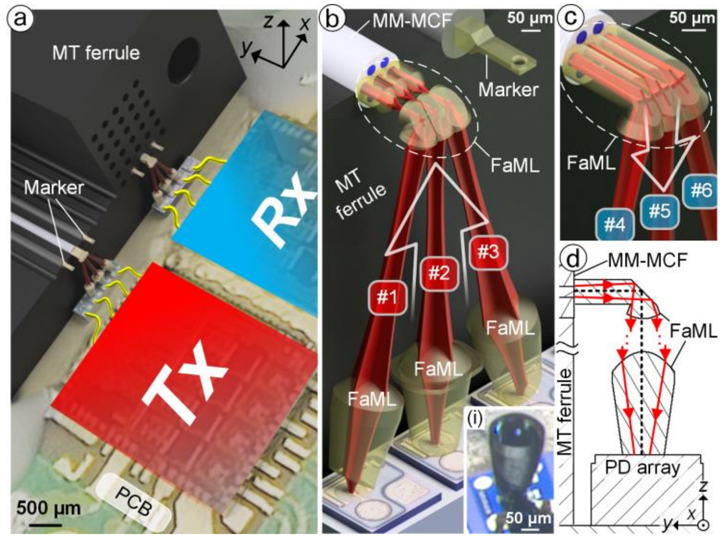

Fig. 1: Concept and implementation of a multi-channel transceiver assembly using seven-core MM-MCF and 3D-printed optical coupling elements. ⓐ The PCB in a QSFP-compatible layout contains two electronic driver IC (Tx, Rx) as well as linear VCSEL and PD arrays which transmit light to or receive light from the MM-MCF. The fibers are glued into an industry-standard MT ferrule. ⓑ Tx coupling structures: The light of each of three VCSEL in a linear array is shaped by 3D-printed facet-attached microlenses (FaML, Inset (i), Channels #1, #2, #3) and sent towards the respective FaML at the Tx fiber facet, where it is redirected by 90° and coupled to one of three horizontally arranged cores of the Tx MM-MCF. 3D-printed marker structures with holes are used to facilitate vision-based passive assembly. To compensate for the pitch mismatch of the MM-MCF cores (39 µm) and VCSEL array (250 µm), the outer FaML (Tx #1, #3) are rotated by 15°. ⓒ Rx coupling structures: 3D-printed FaML located on the Rx MM-MCF redirect the received light (Channels #4, #5, #6) towards three FaML on a linear PD array. The outer FaML (Rx #4, #6) are again rotated by 15°. ⓓ Technical drawing of a cross-section of Channel #5 in ⓒ.

For quantifying the alignment tolerances, we perform an experiment in which we move the MT ferrule in *x*- and *y*-direction, Fig. 1ⓐ, prior to curing the epoxy. By recording the power in Cores #1, #2, #3 of the Tx MM-MCF and by measuring the photocurrents of the Rx PD #4, #5, #6, we find the additional misalignment loss with respect to the optimum position, in which the average power coupled to the Cores #1, #2, #3 of the Tx fiber becomes maximum. The position-dependent misalignment loss along the *x*- and *y*-direction is shown in Fig. 2ⓐ and ⓑ, where the origin corresponds to the optimum position for the three Tx channels. The average 1 dB alignment tolerance, indicated by horizontal dashed lines, amounts to approximately ±18 µm for the *x*- and to ±13 µm for the *y*-direction. To the best of our knowledge, this is the highest alignment tolerance so far demonstrated for coupling to MM-MCF. Note that negative values of *y* would have led to a collision of the MT ferrule with the VCSEL / PD arrays in our experiment, see Fig. 1ⓓ, and were thus not accessible in the measurement. The alignment tolerance along the *y*-direction was estimated by assuming an approximately symmetrical decay of the coupling efficiency. For comparison, the position obtained by the vision-based passive assembly procedure is also indicated in Fig. 2ⓐ and ⓑ, see vertical grey lines ("pass. assy."). The offset between the passively aligned and the optimum position is < 1 µm and < 4 µm in *x*- and *y*-direction, respectively, which is significantly smaller than the corresponding alignment tolerance. This confirms the accuracy of

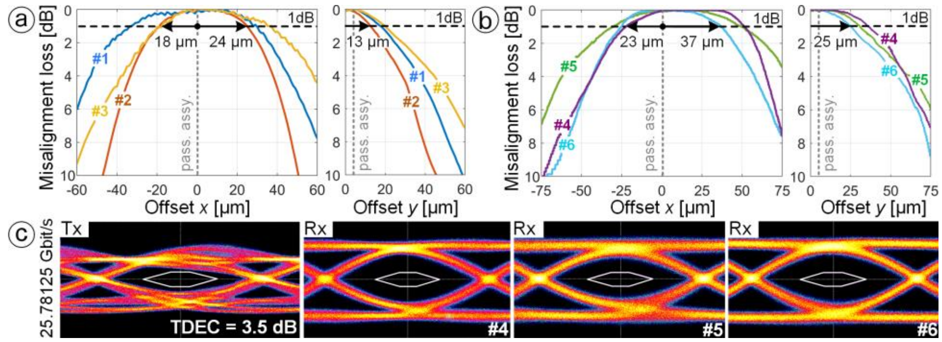

Fig. 2: Characterization and functional demonstration of the three-channel SFP transceiver assembly. ⓐ Tx coupling structure: Measured normalized lateral misalignment loss for an offset along the *x*-axis (left panel) and along the *y*-axis (right panel) for the Tx Channels #1, #2, #3. At the origin, the average power for all three channels reaches a maximum of 2.2 dBm, corresponding to the optimum position of the MT ferrule. With passive assembly (pass. assy.), we hit this position fairly well with an *x*-offset of < 1 µm and a *y*-offset of < 4 µm (vertical dashed lines). In this position, the average coupling loss amounts to 0.7 dB. The average 1 dB alignment tolerance (horizontal dashed line) is ±18 µm for the *x*- and ±13 µm for the *y*-direction. To the best of our knowledge, this corresponds to the highest alignment tolerance so far demonstrated for coupling to MM-MCF. ⓑ Rx coupling structure: Measured normalized lateral misalignment loss for an offset along the *x*-axis (left panel) and along the *y*-axis (right panel) for the Rx channels #4, #5, #6. In the optimum position measured at the Tx, the average Rx coupling loss amounts to 0.6 dB. The average 1 dB alignment tolerance (horizontal dashed line) is ±23 µm for the *x*- and ±25 µm for the *y*-direction. ⓒ Data-transmission experiment at 25.78125 Gbit/s for on-off-keying (OOK) of the VCSEL. Tx: Eye diagram for Channel #2. We find a transmitter-and-dispersion-eye-closure (TDEC) penalty of 3.5 dB, in conformity to IEEE 802.3 specifications. Rx: Eye diagrams for Channels #4, #5, #6.

the passive alignment procedure and of the 3D-printed FaML. At the optimum position, the average power for the VCSEL Channels #1, #2, #3 reaches 2.2 dBm, corresponding to an average coupling loss of 0.4 dB relative to the overall emitted VCSEL power, which was measured by an integrating sphere. With passive assembly, the average power is 1.9 dBm and the weakest channel carries 1.5 dBm, which is in conformity to IEEE 802.3 [10] and which corresponds to an average coupling loss of 0.7 dB. For measuring the absolute losses of the PD Channels #4, #5, #6, we inject a known power into the three Rx fiber cores and use the measured photocurrents along with the data-sheet specification of the responsivity S to extract an average coupling loss of 0.6 dB for both the optimum position and for its passively aligned counterpart. To the best of our knowledge, these results correspond to the lowest coupling loss so far demonstrated for coupling of MM-MCF, outperforming even highly developed molded microlens structures for conventional single-core MMF [11,12].

4. Data-transmission experiments

The transceiver module was characterized according to the industry standard IEEE 802.3 [10]. To this end, we feed the transmitter with an on-off-keying (OOK) signal at a bit rate of 25.78125 Gbit/s, while the optical output from the three transmitter channels is sent to a sampling oscilloscope with an optical front-end. Figure 2ⓒ shows the recorded Tx eye diagram for Channel #2 with a transmitter-and-dispersion-eye-closure (TDEC) penalty of 3.5 dB, in conformity to IEEE 802.3 specifications. For the receiver characterization, the signal from an optical transmitter with known specifications is fed to the MM-MCF, detected by the Rx, and recorded by a sampling oscilloscope connected to an analog output port of the Rx. Figure 2ⓒ shows the Rx eye diagrams for Channels #4, #5, #6.

5. Summary

We have demonstrated a transceiver assembly that relies on 3D-printed optical elements for efficient coupling of MM-MCF to linear VCSEL or PD arrays. The freeform coupling elements are fabricated directly on the fiber and device facets by multi-photon lithography and can be designed to provide large alignment tolerance in a subsequent passive assembly step. We demonstrate record-low coupling losses of 0.7 dB for the transmitter and 0.6 dB for the receiver side. The viability of the concept is demonstrated by integrating the coupling structures into a 3×25 Gbit/s transceiver assembly that is compatible with the space requirements of a small form-factor pluggable (SFP) module.

This work was supported by the BMBF projects PRIMA (# 13N14630), Open6GHub (# 16KISK010) and DiFeMiS (# 16ES0948), which is part of the programme "Forschungslabore Mikroelektronik Deutschland" (ForLab), by the Deutsche Forschungsgemeinschaft (DFG, German Research Foundation) under Germany's Excellence Strategy via the Excellence Cluster 3D Matter Made to Order (EXC-2082/1 – 390761711), by the EU H2020 Photonic Packaging Pilot Line PIXAPP (731954), by the ERC Consolidator Grant "TeraSHAPE" (# 773248), by the Alfried Krupp von Bohlen und Halbach Foundation, and by the Karlsruhe School of Optics & Photonics (KSOP).

References

[1] Puttnam *et al.*, "Space-division Multiplexing for Optical Fiber Communications," Optica **8**, 1186 (2021).
[2] Winzer *et al.*, "From Scaling Disparities to Integrated Parallelism: A Decathlon for a Decade," J. Lightw. Technol. **35**, 1099–1115 (2017).
[3] Gonda *et al.*, "Design of Multicore Fiber Having Upgradability from Standard Single-Mode Fibers and Its Application," J. Lightw. Technol. **37**, 396–403 (2019).
[4] Karppinen *et al.*, "Integration of 150 Gbps/fiber Optical Engines Based on Multicore Fibers and 6-channel VCSELs and PDs," in *Optical Interconnects XVI* (OI 2016), paper 97530S.
[5] Shikama *et al.*, "Multicore-Fiber Receptacle with Compact Fan-In/Fan-Out Device for SDM Transceiver Applications," J. Lightw. Technol. **36**, 5815–5822 (2018).
[6] Puttnam *et al.*, "2.15 Pb/s Transmission Using a 22 Core Homogeneous Single-Mode Multi-Core Fiber and Wideband Optical Comb," in *2015 European Conference on Optical Communication* (ECOC 2015), paper 1056 *(post-deadline)*.
[7] Lee *et al.*, "End-To-End Multicore Multimode Fiber Optic Link Operating up to 120 Gb/s," J. Lightw. Technol. **30**, 886–892 (2012).
[8] Zhu *et al.*, "70-Gb/s Multicore Multimode Fiber Transmissions for Optical Data Links," IEEE Photonics Technol. Lett. **22**, 1647–1649 (2010).
[9] Precitec GmbH & Co. KG, "Optical Sensor CHRocodile S," www.precitec.com/optical-3d-metrology/products/point-sensors/chrocodile-2s/.
[10] "IEEE Standard for Ethernet Amendment 3: Physical Layer Specifications and Management Parameters for 40 Gb/s and 100 Gb/s Operation over Fiber Optic Cables," in *IEEE Std 802.3bm-2015* (2015). www.standards.ieee.org/standard/802_3bm-2015.html.
[11] Nasu *et al.*, "1.3-Tb/s VCSEL-Based On-Board Parallel-Optical Transceiver Module for High-Density Optical Interconnects," J. Lightw. Technol. **36**, 159–167 (2018).
[12] Kuznia *et al.*, "Chip Scale Package Fiber Optic Transceiver Integration for Harsh Environments," in *International Conference on Space Optics* (ICSO 2014), paper 114.